Asian Journal of Control

Hybrid control of synchronization of fractional order nonlinear systems

Journal:	*Asian Journal of Control*
Manuscript ID	RR-17-0775.R3
Wiley - Manuscript type:	Regular issue: Regular paper
Date Submitted by the Author:	12-Feb-2019
Complete List of Authors:	Mohadeszadeh, Milad; Ferdowsi University of Mashhad, Pariz, Naser
Keywords:	finite-time synchronization, sliding mode control, hybrid control, fractional-order derivative, chaotic system, Lyapunov theorem
Abstract:	Under the existence of model uncertainties and external disturbance, finite-time projective synchronization between two identical complex and two identical real fractional-order (FO) chaotic systems are achieved by employing FO sliding mode control approach. In this paper, to ensure the occurrence of synchronization and asymptotic stability of the proposed methods, a sliding surface is designed and the Lyapunov direct method is used. By using integer and FO derivatives of a Lyapunov function, three different FO real and complex control laws are derived. A hybrid controller based on a switching law is designed which has an efficient behavior than the each one of the designed controllers based on the minimization of an appropriate cost function. Numerical simulations are implemented for verifying the effectiveness of the methods.

Hybrid control of synchronization of fractional order nonlinear systems

Milad Mohadeszadeh, Naser Pariz[1]

Department of Electrical Engineering, Ferdowsi University of Mashhad, Iran,

mohadeszadeh@mail.um.ac.ir, n-pariz@um.ac.ir.

Abstract

Under the existence of model uncertainties and external disturbance, finite-time projective synchronization between two identical complex and two identical real fractional-order (FO) chaotic systems are achieved by employing FO sliding mode control approach. In this paper, to ensure the occurrence of synchronization and asymptotic stability of the proposed methods, a sliding surface is designed and the Lyapunov direct method is used. By using integer and FO derivatives of a Lyapunov function, three different FO real and complex control laws are derived. A hybrid controller based on a switching law is designed which has an efficient behavior than the each one of the designed controllers based on the minimization of an appropriate cost function. Numerical simulations are implemented for verifying the effectiveness of the methods.

Keywords: fractional-order derivative; chaotic system; finite-time synchronization; sliding mode control; Lyapunov theorem; hybrid control

1. Introduction

FO calculus attracted considerable attentions in recent years because it has been recently found that several physical phenomena can be more adequately described by FO differential equations rather than integer-order models [1-3], and FO systems can show complex dynamical behavior such as chaos. Memory and more degrees of freedom are the main advantages in FO systems. A

[1] Corresponding author email: n-pariz@um.ac.ir, Tel. +98 513 8805021

less conservative asymptotic stability condition and a new definition for the exponential stability condition of FO systems are investigated in [4]. In [5], using the Lyapunov direct method, a state feedback controller is designed for the stabilization of FO nonlinear systems. The chaotic systems appear in many important fields of engineering such as secure communication [6, 7]; For example, the chaotic systems with complex variables can carry more transmitted information and increase additionally security of information [8]. By separating the real and imaginary parts of FO complex chaotic system, one can obtain the corresponding real one. Several FO complex chaotic systems named such as Lorenz, Chen, T and Lü [9-12], have been proposed. However, there has been little works for synchronization of FO complex chaotic systems; some drawbacks to this problem should be considered. To the best of our knowledge, the control effort problem for the synchronization of such kinds of these systems is not considered and this is the main drawback.

Since pioneering work by Pecora and Carroll [13], chaos synchronization has attracted a lot of significant interests and many published papers have been reported [14-19]. The finite-time synchronization occurs using some control techniques such as sliding mode [16, 18-21] whenever the state trajectories of the slave system should track the state trajectories of the master system in a finite-time. To achieve faster convergence in the real world applications, finite-time control technique is more valuable than infinite-time control technique. The major advantages of sliding-mode control such as easy realization, its robustness to the plant parameters uncertainty and low sensitivity to unknown disturbance make it different from the other control approaches. Most of the literature are focused on the synchronization of FO chaotic systems via the conventional discontinuous-time sliding mode control approach [18, 21]; while the continuous-time sliding mode control is more efficient to reduce the chattering phenomenon [22, 23]. Using the FO calculus and an integral manifold, the chattering phenomena is eradicated in the sliding mode control technique in [24]. In [19], there are some mistakes belong to the calculation of the finite-time for the projective synchronization of different integer-order chaotic systems with model uncertainties and external disturbances; which we will modify them and extend the main results to the FO counterpart. Most of the literatures have been focused on the synchronization of real variable chaotic systems. But in [25], the modified projective synchronization and the modified function projective synchronization of a class of real and complex chaotic systems are studied. If two non-identical real or complex chaotic systems are synchronized, the control effort is high and in the identical case, it degrades significantly. But as a special case in [18], in order to synchronize two non-identical real chaotic systems, a little control effort is required. A switched system is a kind of hybrid system that consists of a number of subsystems and a switching law determining at any time instant which subsystem operates [26]. A different switching law will cause different system performance. Hybrid systems arise in the application of multiple controllers which have been widely used in many cases such as adaptive control, multi-agent systems and so on.

According to the above discussion, the main contribution of this paper is designing a new hybrid FO controller for the finite-time synchronization of a general class of FO chaotic systems which its calculation process contains new idea. Also, two different scheme is accomplished to verify the stability of the closed-loop system.

The rest of this paper is organized as follows. First, the preliminaries of FO calculus are introduced. Then, the system description and problem statement are given. After that, the design strategy of the proposed control approach is presented, and finally, some conclusions are reviewed.

1. Preliminaries of FO systems

The FO integration of an appropriate continuous function is as [1]

$$ {}_{t_0}D_t^{-\alpha} f(t) = \frac{1}{\Gamma(\alpha)} \int_{t_0}^{t} \frac{f(\tau)}{(t-\tau)^{1-\alpha}} d\tau,\ f(t): R^+ \to R \tag{1} $$

where $\Gamma(z)=\int_{t_0}^{\infty} t^{z-1} e^{-t} dt$. The Caputo FO derivative of a continuous function, defined by [1]

$$ {}_{t_0}D_t^{\alpha} f(t) = \frac{1}{\Gamma(m^* - \alpha)} \int_0^t \frac{f^{(m^*)}(\tau)}{(t-\tau)^{\alpha+1-m^*}} d\tau \tag{2}$$

where m^* is the first integer larger than $\alpha \in R^+$.

Definition 1. [1]. The Mittag-Leffler function is defined as

$$E_{\alpha,\beta}(z) = \sum_{k=0}^{\infty} \frac{z^k}{\Gamma(k\alpha+\beta)}, \quad (\alpha,\beta) > 0 \tag{3}$$

We know that [1]

$$\int_0^{\infty} e^{-St} t^k e^{\pm \nu t} dt = \frac{k!}{(S \mp \nu)^{k+1}} . \tag{4}$$

Using (3) and (4), one can obtain [1]

$$L\{t^{\alpha k+\beta-1} E_{\alpha,\beta}^{(k)}(\pm \nu t^{\alpha})\} = \frac{k! S^{\alpha-\beta}}{(S^{\alpha} \mp \nu)^{k+1}}, \tag{5}$$

where S is a variable in the frequency domain and $R(S)$ denotes the real part of S, $R(S) > |\nu|^{1/\alpha}$, $\nu \in R$.

We will use the following equality with $\beta > 0$ [1]

$$\int_0^z E_{\alpha,\beta}(\mp \nu t^{\alpha}) t^{\beta-1} dt = z^{\beta} E_{\alpha,\beta+1}(\mp \nu z^{\alpha}) \tag{6}$$

In this paper, the operator ${}_{t_0}D_t^{\alpha}$ is called ''α-order Caputo differential operator''. Also, the Adams-Bashforth-Moulton algorithm is used with a step size $h = 0.001$ for solving FO differential equations [27].

2. Problem formulation

The n-dimensional FO complex chaotic system is considered as

$$ {}_{t_0}D_t^{\alpha} x = \mathcal{F}(x) + \Delta\mathcal{F}(x) + d^x(t) \tag{7}$$

In this case, $\alpha \in (0,1)$ is the FO operator, $x = (x_1,x_2,...,x_n)^T \in C^n$ is the complex state vector of the drive system, $x = x^r + jx^i$, $j = \sqrt{-1}$, $x^r = (m_1,m_3,...,m_{2n-1})^T$, $x^i = (m_2,m_4,...,m_{2n})^T$, $\mathcal{F}(x) = \mathcal{F}^r(x) + j\mathcal{F}^i(x) = (\mathcal{F}_1(x),\mathcal{F}_2(x),...,\mathcal{F}_n(x))^T \in C^n$ is the complex continues nonlinear vector functions, $\mathcal{F}^r(x) = (f_1(x),f_3(x),...,f_{2n-1}(x))^T$, $\mathcal{F}^i(x) = (f_2(x),f_4(x),...,f_{2n}(x))^T$. $\Delta\mathcal{F}(x) = \Delta\mathcal{F}^r(x) + j\Delta\mathcal{F}^i(x) = (\Delta\mathcal{F}_1(x),\Delta\mathcal{F}_2(x),...,\Delta\mathcal{F}_n(x))^T \in C^n$ is the vector of system uncertainties, $\Delta\mathcal{F}^r(x) = (\Delta f_1(x),\Delta f_3(x),...,\Delta f_{2n-1}(x))^T$, $\Delta\mathcal{F}^i(x) = (\Delta f_2(x),\Delta f_4(x),...,\Delta f_{2n}(x))^T$. $d^x(t) = d^{x,r}(t) + j d^{x,i}(t) \in C^n$ is the vector of external disturbances, $d^{x,r}(t) = (d_1^x,d_3^x,...,d_{2n-1}^x)^T$, $d^{x,i}(t) = (d_2^x,d_4^x,...,d_{2n}^x)^T$.

and the controlled response system can be described as

$${}_{t_0}D_t^{\alpha} y = \mathbb{G}(y) + \Delta\mathbb{G}(y) + d^y(t) - u(t) \tag{8}$$

where $y = (y_1,y_2,...,y_n)^T$ is the complex state vector of the response system, $y = y^r + jy^i$, $y^r = (r_1,r_3,...,r_{2n-1})^T$, $y^i = (r_2,r_4,...,r_{2n})^T$, $\mathbb{G}(y) = \mathbb{G}^r(y) + j\mathbb{G}^i(y) = (\mathbb{G}_1(y),\mathbb{G}_2(y),...,\mathbb{G}_n(y))^T \in C^n$ is the complex continues nonlinear vector functions, $\mathbb{G}^r(y) = (g_1(y),g_3(y),...,g_{2n-1}(y))^T$, $\mathbb{G}^i(y) = (g_2(y),g_4(y),...,g_{2n}(y))^T$. $\Delta\mathbb{G}(y) = \Delta\mathbb{G}^r(y) + j\Delta\mathbb{G}^i(y) = (\Delta\mathbb{G}_1(y),\Delta\mathbb{G}_2(y),...,\Delta\mathbb{G}_n(y))^T \in C^n$ is the vector of system uncertainties, $\Delta\mathbb{G}^r(y) = (\Delta g_1(y),\Delta g_3(y),...,\Delta g_{2n-1}(y))^T$, $\Delta\mathbb{G}^i(y) = (\Delta g_2(y),\Delta g_4(y),...,\Delta g_{2n}(y))^T$. $d^y(t) = d^{y,r}(t) + jd^{y,i}(t) \in C^n$ is the vector of external disturbances, $d^{y,r}(t) = (d_1^y,d_3^y,...,d_{2n-1}^y)^T$, $d^{y,i}(t) = (d_2^y,d_4^y,...,d_{2n}^y)^T$. $u = (u_1,u_2,...,u_n)^T = u^r + ju^i$ is the complex control input vector to be designed later, $u^r = (v_1,v_3,...,v_{2n-1})^T$, $u^i = (v_2,v_4,...,v_{2n})^T$.

Define the error state vector as

$$\delta = \delta^r + j\delta^i = y - \Xi\, x \tag{9}$$

where $\delta = (\delta_1,\delta_2,...,\delta_n)^T$, $\delta^r = (e_1,e_3,...,e_{2n-1})^T$, $\delta^i = (e_2,e_4,...,e_{2n})^T$ is the synchronization error vector, $\Xi = \Xi^r + j\Xi^i = diag(\Xi_1,\Xi_2,...,\Xi_n)$ is the $(n \times n)$ diagonal complex scaling matrix, $\Xi^r = diag(\Lambda_1,\Lambda_3,...,\Lambda_{2n-1})$, $\Xi^i = diag(\Lambda_2,\Lambda_4,...,\Lambda_{2n})$.

Remark 1. In this paper, we define $\|s\| = \sqrt{{s_1}^2 + {s_2}^2 + ... + {s_n}^2}$ and $\|s\|_1 = |s_1| + |s_2| + ... + |s_n|$; where $s = (s_1, s_2,...,s_n)^T$ is a vector of continuous functions.

Remark 2. For convenience, from now on, $\mathcal{F}$,$\Delta\mathcal{F}$,$\mathbb{G}$,$\Delta\mathbb{G}$, d^x,d^y, Δ stand for $\mathcal{F}(x)$,$\Delta\mathcal{F}(x)$,$\mathbb{G}(y)$,$\Delta\mathbb{G}(y)$, $d^x(t)$,$d^y(t)$, $(\delta + \|\delta\|^{-2\beta}\delta)$, respectively.

Using (7-9), the error dynamic is yielded as

$$ {}_{t_0}D_t^{\alpha}\delta = \mathbb{G} - \Xi\,\mathcal{F} + \Delta\mathbb{G} - \Xi\,\Delta\mathcal{F} + d^y - \Xi\,d^x - u \tag{10} $$

By separating the real and imaginary parts of (10)

$$ \begin{cases} {}_{t_0}D_t^{\alpha}\delta^r = \mathbb{G}^r - (\Xi^r\,\mathcal{F}^r - \Xi^i\,\mathcal{F}^i) \\ \quad + \Delta\mathbb{G}^r - (\Xi^r\,\Delta\mathcal{F}^r - \Xi^i\,\Delta\mathcal{F}^i) \\ \quad + d^{y,r} - (\Xi^r\,d^{x,r} - \Xi^i\,d^{x,i}) - u^r, \\ {}_{t_0}D_t^{\alpha}\delta^i = \mathbb{G}^i - (\Xi^r\,\mathcal{F}^i + \Xi^i\,\mathcal{F}^r) \\ \quad + \Delta\mathbb{G}^i - (\Xi^r\,\Delta\mathcal{F}^i + \Xi^i\,\Delta\mathcal{F}^r) \\ \quad + d^{y,i} - (\Xi^r\,d^{x,i} + \Xi^i\,d^{x,r}) - u^i \end{cases} \tag{11} $$

Definition 2. It is said that hybrid complex projective synchronization occurs between the drive system (7) and the response system (8) with a diagonal complex scaling matrix $\Xi = \Xi^r + j\Xi^i$, in a finite-time, if there exist a complex controller vector $u = u^r + ju^i$ such that

$$ \lim_{t \to T} \delta = \lim_{t \to T} \|y - \Xi\,x\| = 0,\; t > T \tag{12} $$

The discussion of the hybrid complex projective synchronization between two FO complex chaotic systems (7) and (8) can be translated into the analysis of the asymptotical stability of the zero solution of the error system (10).

Assumption 1. The uncertainties and external disturbances are assumed to be bounded. Therefore, there exist appropriate positive constants θ_k,θ'_k, Θ_k,Θ'_k, ε_k, ε'_k,ϵ_k,ϵ'_k, $k = 1,2,\dots,2n$ such that:

$$\begin{cases} |\Delta f_k| < \theta_k \,, |\Delta g_k| < \Theta_k, \\ |d_k^x| < \varepsilon_k \,, |d_k^y| < \epsilon_k, \\ \left|{}_{t_0}D_t^{1-\alpha}\Delta f_k\right| < \theta'_k \,, \left|{}_{t_0}D_t^{1-\alpha}\Delta g_k\right| < \Theta'_k, \\ \left|{}_{t_0}D_t^{1-\alpha}d_k^x\right| < \varepsilon'_k \,, \left|{}_{t_0}D_t^{1-\alpha}d_k^y\right| < \epsilon'_k \end{cases} \tag{13}$$

Hence, one can conclude from (13)

$$\begin{cases} |\Delta g_k - (\Lambda_k \,\Delta f_k - \Lambda_{k+1} \,\Delta f_{k+1})| < \tau_k, \\ \left|d_k^y - \left(\Lambda_k \, d_k^x - \Lambda_{k+1} \, d_{k+1}^x\right)\right| < \chi_k, \\ \left|{}_{t_0}D_t^{1-\alpha}(\Delta g_k - (\Lambda_k \,\Delta f_k - \Lambda_{k+1} \,\Delta f_{k+1}))\right| < \tau'_k, \\ \left|{}_{t_0}D_t^{1-\alpha}\left(d_k^y - \left(\Lambda_k \, d_k^x - \Lambda_{k+1} \, d_{k+1}^x\right)\right)\right| < \chi'_k, \\ \qquad k = 1,3,\dots,2n-1 \end{cases} \tag{14}$$

$$\begin{cases} |\Delta g_k - (\Lambda_k \,\Delta f_{k-1} + \Lambda_{k-1} \,\Delta f_k)| < \tau_k, \\ \left|d_k^y - \left(\Lambda_k \, d_{k-1}^x + \Lambda_{k-1} \, d_k^x\right)\right| < \chi_k, \\ \left|{}_{t_0}D_t^{1-\alpha}(\Delta g_k - (\Lambda_k \,\Delta f_{k-1} + \Lambda_{k-1} \,\Delta f_k))\right| < \tau'_k, \\ \left|{}_{t_0}D_t^{1-\alpha}\left(d_k^y - \left(\Lambda_k \, d_{k-1}^x + \Lambda_{k-1} \, d_k^x\right)\right)\right| < \chi'_k, \\ \qquad k = 2,4,\dots,2n \end{cases} \tag{15}$$

where τ_k, χ_k, τ'_k, χ'_k, $k = 1,2,\dots,2n$ are positive constants.

Lemma 1. For every given scalar Φ and positive scalar Ψ, the following inequality holds: [28]

$$\Phi \, tanh(\Psi\Phi) = |\Phi||tanh(\Psi\Phi)| \geq 0 \tag{16}$$

Lemma 2. (Barbalat's lemma [29]). If η:$R\rightarrow R$ is a uniformly continuous function for $t \geq 0$ and if the limit of $\int_0^t \eta(\omega)d\omega$ exists and is finite, then $\lim_{t\to\infty} \eta(t) = 0$.

3. Controller design

In our proposed sliding mode control scheme, first we consider a sliding function based on the desired system dynamics as [19]

$$s = \delta + \rho\int_0^t (\delta + \|\delta\|^{-2\beta}\delta)dt \tag{17}$$

where $s = s^r + js^i = (s_1, s_2, \ldots, s_n)^T \in C^n$, $\rho > 0$ and $\beta \neq 0$.

Therefore one gets

$$\begin{cases} s^r = \delta^r + \rho\int_0^t(\delta^r + \|\delta\|^{-2\beta}\delta^r)dt \\ s^i = \delta^i + \rho\int_0^t(\delta^i + \|\delta\|^{-2\beta}\delta^i)dt \end{cases} \tag{18}$$

where $s^r = (\sigma_1, \sigma_3, \ldots, \sigma_{2n-1})^T$, $s^i = (\sigma_2, \sigma_4, \ldots, \sigma_{2n})^T$.

Once the system operates in the sliding motion, it satisfies $\dot{s} = 0$ [29].

Hence (18) can be obtain as

$$\begin{cases} \dot{\delta}^r = -\rho(\delta^r + \|\delta\|^{-2\beta}\delta^r) \\ \dot{\delta}^i = -\rho(\delta^i + \|\delta\|^{-2\beta}\delta^i) \end{cases} \tag{19}$$

Theorem 3.1. The sliding mode dynamic (19) is finite-time stable; i.e., the states of (19) will converge to the zero equilibrium $e_k = 0$, $k = 1,2,\ldots,2n$ from $t \geq T_1$; where T_1 is as

$T_1 \leq 1/2\rho\beta\left(1 + \left(\sum_{k=1}^{2n} e_k(0)^2\right)^\beta\right)$.

Proof. Consider a Lyapunov function as $V_1 = 1/2\sum_{k=1}^{2n} {e_k}^2$ and taken its time derivative

$$\dot{V}_1 = -\rho\sum_{k=1}^{2n} e_k\left(e_k + \|\delta\|^{-2\beta}e_k\right) \tag{20}$$

Hence one can conclude that

$$\dot{V}_1 = -2\rho V_1 - 2^{1-\beta}\rho {V_1}^{-\beta} V_1 \tag{21}$$

Multiplying (21) by $\beta {V_1}^{\beta-1}e^{2\rho\beta t}$, it yields

$$\left(\beta {V_1}^{\beta-1}\dot{V}_1 + 2\rho\beta {V_1}^\beta\right)e^{2\rho\beta t} = -2^{1-\beta}\rho\beta e^{2\rho\beta t} \tag{22}$$

where e is an exponential function. Then one obtains

$$\frac{d}{dt}\left({V_1}^\beta e^{2\rho\beta t}\right) = -2^{1-\beta}\rho\beta e^{2\rho\beta t} \tag{23}$$

Integrating from both sides of (23) from zero to t

$$V_1(t)^\beta = \left(2^{-\beta} + V_1(0)^\beta\right)e^{-2\rho\beta t} - 2^{-\beta} \tag{24}$$

Hence, the states e_k will converge to zero in a finite-time

$$T_1 = t \leq {}^{1}/_{2\rho\beta} ln\left(1 + \left(\sum_{k=1}^{2n} e_k(0)^2\right)^{\beta}\right) \tag{25}$$

Thus, the proof is achieved completely.

After designing the sliding manifold, the next step is to design the reasonable control law to force the error trajectories to go onto the sliding surface within the finite-time. In order to assure the existence of the sliding motion (to satisfy the reaching condition $s^T\dot{s} \leq 0$) and to eliminate the chattering phenomenon caused by the sign function, a continuous control law is proposed as

$$\begin{cases} v_k = g_k - (\Lambda_k f_k - \Lambda_{k+1} f_{k+1}) + \\ {}_{t_0}D_t^{\alpha-1}\left(\rho\left(e_k + \|\delta\|^{-2\beta} e_k\right) + \omega\, tanh(\eta\, \sigma_k) + \lambda\, \sigma_k\right), \\ \qquad k = 1,3,\ldots,2n-1 \\ v_k = g_k - (\Lambda_k f_{k-1} + \Lambda_{k-1} f_k) + \\ {}_{t_0}D_t^{\alpha-1}\left(\rho\left(e_k + \|\delta\|^{-2\beta} e_k\right) + \omega\, tanh(\eta\, \sigma_k) + \lambda\, \sigma_k\right), \\ \qquad k = 2,4,\ldots,2n \end{cases} \tag{26}$$

In (26), ω and η are the adaptation coefficients which tune the gain and steepness of the $tanh$ function, respectively. Also λ is a positive gain which tunes the speed of the synchronization.

Theorem 3.2. If the FO chaotic system (11) is controlled by the control law (26), then the system trajectories will tend to the sliding surface $\sigma_k = 0$, $k = 1,2,\ldots,2n$.

Proof. Constructing a Lyapunov function candidate as

$$V_2 = ({}^{1}/2)\left(\sum_{k=1}^{2n} {\sigma_k}^2\right) \tag{27}$$

Taken integer-order derivative from (27) along the trajectories of (17) one obtains

$$\dot{V}_2 = \sum_{k=1}^{2n} \sigma_k\left(\dot{e}_k + \rho\left(e_k + \|\delta\|^{-2\beta} e_k\right)\right) \tag{28}$$

Substituting (11) into (28) results

$$\dot{V}_2 = \sum_{k=1,3}^{2n-1}\sigma_k$$
$$\left({}_{t_0}D_t^{1-\alpha}\left(g_k - \left(\Lambda_k\, f_k - \Lambda_{k+1}\, f_{k+1}\right) + \Delta g_k - \left(\Lambda_k\, \Delta f_k - \Lambda_{k+1}\, \Delta f_{k+1}\right) + d_k^y - \left(\Lambda_k\, d_k^x - \Lambda_{k+1}\, d_{k+1}^x\right) - v_k\right) + \rho\right.$$
$$+ \sum_{k=2,4}^{2n}\sigma_k$$
$$\left({}_{t_0}D_t^{1-\alpha}\left(g_k - \left(\Lambda_k\, f_{k-1} + \Lambda_{k-1}\, f_k\right) + \Delta g_k - \left(\Lambda_k\, \Delta f_{k-1} + \Lambda_{k-1}\, \Delta f_k\right) + d_k^y - \left(\Lambda_k\, d_{k-1}^x + \Lambda_{k-1}\, d_k^x\right) - v_k\right) + \rho\right.$$

(29)

Using the Assumption 1 and inserting (26) into (29), yields

$$\dot{V}_2 \le \sum_{k=1}^{2n} 2(\tau'_k + \chi'_k)\sigma_k - \omega\, \sigma_k\, tanh(\eta\, \sigma_k) - \lambda\, {\sigma_k}^2 \tag{30}$$

Using the Lemma 1, $\sum_{k=1}^{2n}\omega\, \sigma_k\, tanh(\eta\, \sigma_k) = \sum_{k=1}^{2n}\omega\, |\sigma_k||tanh(\eta\, \sigma_k)|$. Thus we have

$$\dot{V}_2 \le \sum_{k=1}^{2n}\left(2(\tau'_k + \chi'_k)\sigma_k - \nu\, |\sigma_k| - \lambda\, {\sigma_k}^2\right) \tag{31}$$

If $\nu \ge \left(2(\tau'_k + \chi'_k) + \xi\right)$, $k = 1,2,\ldots,2n$, where ξ is a positive constants, then

$$\dot{V}_2 \le -\sqrt{2}\xi\, {V_2}^{0.5} - 2\lambda\, V_2 \tag{32}$$

Therefore, the right hand side of (32) is negative semi-definite. So the stability of the system is guaranteed.

Multiplying both sides of (32) by ${V_2}^{-0.5}$, results

$${V_2}^{-0.5}\dot{V}_2 + 2\lambda\, {V_2}^{0.5} \le -\sqrt{2}\xi \tag{33}$$

Multiplying (33) by $(1/2)e^{\lambda t}$ and then integrating at both sides from zero to *t*, one obtains

$${V_2}^{0.5} \le \left((1/\sqrt{2})\,(\xi/\lambda) + V_2(0)^{0.5}\right)e^{-\lambda t} - (1/\sqrt{2})\,(\xi/\lambda)$$

$$T_2 = t \le (1/\lambda)\, ln\left(1 + (\lambda/\xi)\left|\sum_{k=1}^{2n}\sigma_k(0)\right|\right). \tag{34}$$

Therefore, from (32-34) and by directly according to definition 2, the state trajectories of the error system (10) will converge to $\sigma_k = 0$, $k = 1,2,\ldots,2n$ in a finite-time T_2.

According to Theorems 3.1 and 3.2, the finite-time synchronization between the drive system (7) and the response system (8) can be reached in a finite-time $T \leq T_1 + T_2$.

Based on the sliding manifold (17), the different control law will design through the use of FO derivative of the Lyapunov function and the Lemma which proved in [30].

Therefore, in order to assure the existence of the sliding motion ($s^T{}_{t_0}D_t^\alpha s \leq 0$), an appropriate continuous control law is designed as

$$u = \mathbb{G} - \Xi\,\mathcal{F} + \rho\;{}_{t_0}D_t^{\alpha-1}(\Delta) + \omega\,tanh(\eta\,s) + \lambda\,s \tag{35}$$

Theorem 3.3. If the FO chaotic system (11) is controlled by the control law (35), then the system trajectories will tend to the sliding surface $s = 0$.

Proof. Construct a Lyapunov function candidate as $V_3 = s^T s/2$.

Taken FO derivative from Lyapunov function along the trajectories of (17), yields

$${}_{t_0}D_t^\alpha V_3 \leq s^T\big(\mathbb{G} - \Xi\,\mathcal{F} + \Delta\mathbb{G} - \Xi\,\Delta\mathcal{F} + d^y - \Xi\,d^x - u + \rho_{t_0}D_t^{\alpha-1}(\Delta)\big) \tag{36}$$

According to the Assumption 1 and inserting the control input (35) into (36), one has

$${}_{t_0}D_t^\alpha V_3 \leq (\tau + \chi)\|s\|_1 - \omega\,s^T\,tanh(\eta\,s) - \lambda\,\|s\|^2$$

We assume $\omega\,s^T\,tanh(\eta\,s) = \nu\,\|s\|_1$. Thus one can conclude that

$${}_{t_0}D_t^\alpha V_3 \leq K\|s\|_1 - \lambda\,\|s\|^2 \leq (K - \lambda)\,\|s\|^2$$

where $K = (\tau + \chi - \omega)$. If $K - \lambda \leq -L$, then

$${}_{t_0}D_t^\alpha V_3 \leq -2L\,V_3 \tag{37}$$

Therefore, the right hand side of (37) is negative semi-definite. So the stability of system is guaranteed. Using the Volterra integral

$$V_3(t) - \sum_{k=0}^{\lceil\alpha\rceil-1} V_3(t_0)^{(k)}\frac{t^k}{k!} \leq -\frac{2L}{\Gamma(\alpha)}\int_0^t \frac{V_3(\tau)}{(t-\tau)^{1-\alpha}}d\tau \tag{38}$$

let $\sum_{k=0}^{\lceil\alpha\rceil-1} V_3(t_0)^{(k)}\frac{t^k}{k!} = V_3(t_0)$, the inequality (38) can be rewritten as

$$\frac{2L}{\Gamma(\alpha)}\int_0^t \frac{V_3(\tau)}{(t-\tau)^{1-\alpha}}d\tau \le V_3(t_0) - V_3(t)$$

Since ${}_{t_0}D_t^{\alpha}V_3 \le 0$ and $V_3(t_0) - V_3(t) \ge 0$ is positive and finite, one can obtain that $\frac{2L}{\Gamma(\alpha)}$ $\int_0^t \frac{V_3(\tau)}{(t-\tau)^{1-\alpha}}d\tau$ exists and is finite. Thus according to Lemma 2, $\lim_{t\to\infty} V_3(t) = 0$.

Therefore $s\to 0$. Thus, the system trajectories can be driven onto the predefined sliding surface and the proof is completed.

Moreover, a different finite-time FO control law is designed as

$$u = \mathbb{G} - \Xi\,\mathcal{F} + \delta + \rho\,{}_{t_0}D_t^{1-\alpha}\left({}_{t_0}D_t^{2\alpha-2}(\Delta) + {}_{t_0}D_t^{\alpha-2}(\Delta)\right) + s\left(s^T s\right)^{-q} - \frac{\varepsilon\, s}{\|s\|^2} \tag{39}$$

where q is not zero and ε is a positive constant.

Theorem 3.4. If the FO chaotic system (10) is controlled by the control law (39), then the system trajectories will tend to the sliding surface $s = 0$ in a finite-time.

Proof. Constructing a quadratic Lyapunov function as $V_4 = \frac{(s^T s)}{2}$.

Taken FO derivative of the Lyapunov function along the trajectories of (17) one obtains

$${}_{t_0}D_t^{\alpha}V_4 \le s^T\left({}_{t_0}D_t^{\alpha}\delta + \rho\,{}_{t_0}D_t^{\alpha-1}(\Delta)\right)^T \tag{40}$$

Substituting (10) into (40) and then using the control input (39) yields

$${}_{t_0}D_t^{\alpha}V_4 \le s^T\left(\Delta\mathbb{G} - \Xi\,\Delta\mathcal{F} + d^y - \Xi\, d^x - s - s\left(s^T s\right)^{-q} + \frac{\varepsilon\, s}{\|s\|^2}\right)$$

According to the Assumption 1, ${}_{t_0}D_t^{\alpha}V_4 \le -\|s\|^2 - \|s\|^{2-2q} + \|s\|^2(\tau + \chi) + \varepsilon$.

If $(\tau + \chi - 1) \le -\nu$, where ν is a positive constants, then

$${}_{t_0}D_t^{\alpha}V_4 \le -2\nu\, V_4 - 2^{1-q}{V_4}^{1-q} + \varepsilon \le -2\nu\, V_4 + \varepsilon \tag{41}$$

Taken the Laplace transform from (41) with respect to $V_4(0) = 0$, we have $V_4(S) = \frac{\varepsilon}{S(S^{\alpha} + 2\nu)}$.

Using definition 1 and equality (5), then $V_4(t)$ obtains as, $V_4(t) = \varepsilon\int_0^t t^{\alpha-1}E_{\alpha,\alpha}(-2\nu\, t^{\alpha})dt$.

Based on the equality (6), it follows that

$$V_4(t) \le \varepsilon\, t^{\alpha}E_{\alpha,\alpha+1}(-2\nu\, t^{\alpha}) \le \varepsilon\sum_{k=0}^{\infty}\frac{(-1)^k(2\nu)^k t^{\alpha k}}{\Gamma((k+1)\alpha+1)} \tag{42}$$

Thus, by simple calculation, one can conclude that the right hand side of (42) is convergent which implies that the state trajectories in (17) converge to $s = 0$. Therefore, the proof is completed.

4. Numerical simulation and experimental results

Case 1: Finite-time synchronization of FO complex chaotic Chen systems

According to the results in section 3, in this example, the complex projective synchronization between two identical FO complex chaotic Chen systems [10] with different initial conditions in the presence of system uncertainties and external disturbances will study. The drive system is as

$${}_{t_0}D_t^{\alpha}x = \underbrace{\begin{pmatrix} 35(x_2 - x_1) \\ -7x_1 + 28x_2 - x_1x_3 \\ {}^1\!/_2(\bar{x}_1x_2 + x_1\bar{x}_2) - 3x_3 \end{pmatrix}}_{\mathcal{F}} + \underbrace{\begin{pmatrix} A(\sin(m_1) + j\cos(m_2)) \\ A(\sin(m_3) + j\cos(m_4)) \\ A\sin(m_5) \end{pmatrix}}_{\Delta\mathcal{F}} + \underbrace{\begin{pmatrix} A(\sin(t) + j\cos(t)) \\ A(\sin(t) + j\cos(t)) \\ A\sin(t) \end{pmatrix}}_{d^x} \tag{43}$$

and the uncontrolled response system can be as

$${}_{t_0}D_t^{\alpha}y = \underbrace{\begin{pmatrix} 35(y_2 - y_1) \\ -7y_1 + 28y_2 - y_1y_3 \\ {}^1\!/_2(\bar{y}_1y_2 + y_1\bar{y}_2) - 3y_3 \end{pmatrix}}_{\mathcal{F}} + \underbrace{\begin{pmatrix} A(\cos(r_1) + j\sin(r_2)) \\ A(\cos(r_3) + j\sin(r_4)) \\ A\cos(r_5) \end{pmatrix}}_{\Delta\mathbb{G}} + \underbrace{\begin{pmatrix} A(\cos(t) + j\sin(t)) \\ A(\cos(t) + j\sin(t)) \\ A\cos(t) \end{pmatrix}}_{d^y} \tag{44}$$

where A = 0.2. The system exhibits a chaotic behavior when ($\alpha = 0.96$). The parameter of the controller are set as $\rho = 5$, $\beta = 0.1$, $\eta = 0.1$, $\omega = 10$, $\lambda = 10$. $\Xi = diag(1-j, 1-j, 1)$. The initial values of the states of drive and response systems are $(x_1(0), x_2(0), x_3(0))^T = (1 + j1.7,\ 1.3 + j0.5,\ 2.3)^T$ and $(y_1(0), y_2(0), y_3(0))^T = (2 + j0.7,\ 0.5 + j1.6,\ 1.1)^T$, respectively. The synchronized states and the synchronization errors between two systems are shown in Fig. 1 and 2. The time history of the control inputs (26) are depicted in Fig. 3.

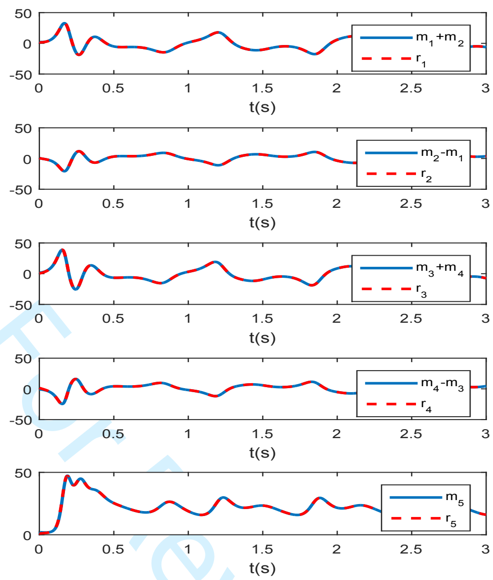

Fig. 1. The synchronized states of the two identical FO complex chaotic Chen systems.

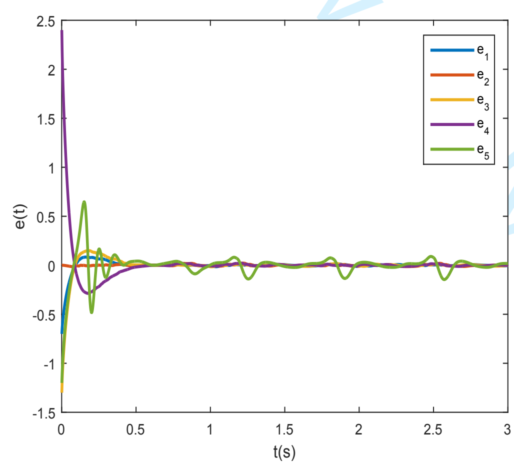

Fig. 2. The synchronization errors between the system (43) and the system (44).

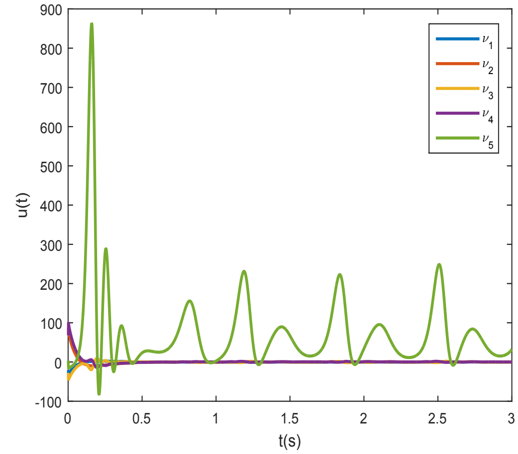

Fig. 3. The time history of the control inputs (26).

Remark 3. As illustrated in Figure 3, the control effort is not sub-optimal. Therefore, to have sub-optimal control of the synchronization of such FO complex chaotic systems, the traditional control techniques like sliding mode control cannot be used. For each synchronization scheme such as hybrid complex projective synchronization with different scaling matrices, the result of the control input is not better than in Figure 3. So, in order to compare the simulation results numerically with the different designed control inputs, a sub-optimal control effort is required in the output of the synchronization system. Therefore, the real counterpart of these systems must be used as an alternative system for the synchronization which has better results and sub-optimal control effort.

Case 2: Hybrid control of synchronization of FO real chaotic Chen systems

In order to design the hybrid control scheme, the following intermediate variables are introduced:

$$\begin{cases} D_1 = \{\delta \in R^3 |\ \|\delta\| \geq Q\} \\ D_2 = \delta \in R^3 |\ \delta \notin D_1 \end{cases} \tag{45}$$

where $\delta = [\delta_1, \delta_2, \delta_3]^T$. The FO controllers defined in (35) and (39) are considered as u_1 and u_2, respectively. The switched error system can be proposed as

$${}_{t_0}D_t^{\alpha}\delta = \mathbb{G} - \mathit{\Xi}\,\mathcal{F} + \Delta\mathbb{G} - \mathit{\Xi}\,\Delta\mathcal{F} + d^y - \mathit{\Xi}\,d^x - u_\sigma \tag{46}$$

where $\sigma = 1$, if $\delta \in D_1$ and $\sigma = 2$, if $\delta \in D_2$. In this case, the complete synchronization between two identical FO real chaotic Chen systems [31] with different initial conditions in the presence of system uncertainties and external disturbances is considered. The drive system is as

$$ {}_{t_0}D_t^{\alpha} x = \underbrace{\begin{pmatrix} 35(x_2 - x_1) \\ -7\,x_1 - x_1 x_3 + 28\,x_2 \\ x_1 x_2 - 3x_3 \end{pmatrix}}_{\mathcal{F}} + \underbrace{\begin{pmatrix} A(\cos(x_1) + \sin(2t)) \\ A(\cos(x_2) + \sin(2t)) \\ A(\cos(x_3) + \sin(2t)) \end{pmatrix}}_{\Delta\mathcal{F} + d^x} \tag{47} $$

and the uncontrolled response system is as

$$ {}_{t_0}D_t^{\alpha} y = \underbrace{\begin{pmatrix} 35(y_2 - y_1) \\ -7y_1 - y_1 y_3 + 28y_2 \\ y_1 y_2 - 3y_3 \end{pmatrix}}_{\mathcal{F}} + \underbrace{\begin{pmatrix} A(\sin(y_1) + \cos(2t)) \\ A(\sin(y_2) + \cos(2t)) \\ A(\sin(y_3) + \cos(2t)) \end{pmatrix}}_{\Delta\mathbb{G} + d^y} \tag{48} $$

where A=0.2. The system exhibits a chaotic behavior when $\alpha = 0.9$. The parameter of the controller are set as $Q = 0.07, \rho = 5,\ \beta = 0.1,\ \eta = 0.1,\ \omega = 10,\ \lambda = 10$ and $\Xi = diag(1,1,1)$. Parameter Q is acquired by the trial and error procedure in order to minimize the cost function. The initial conditions of states are $(x_1(0), x_2(0), x_3(0))^T = (1.5, 0.1, 1.7)^T$ and $(y_1(0), y_2(0), y_3(0))^T = (0.5, 1.4, 0.2)^T$. The synchronized states and the synchronization errors between (47) and (48) are shown in Fig. 4 and Fig. 5, respectively. The hybrid control input signal under the switching law (45) is depicted in Fig. 6.

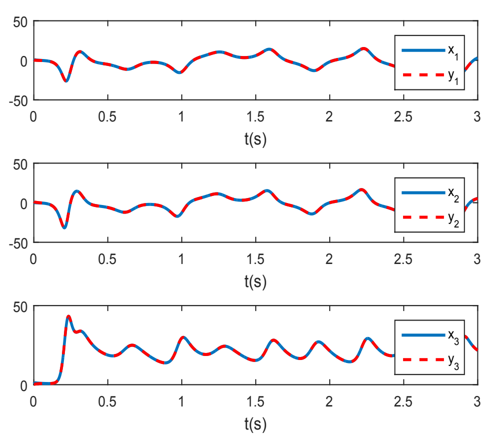

Fig. 4. The synchronized sates of the system (47) and the system (48).

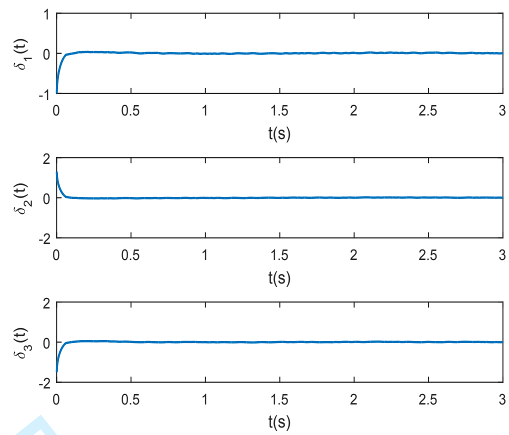

Fig. 5. The synchronization errors between the system (47) and the system (48).

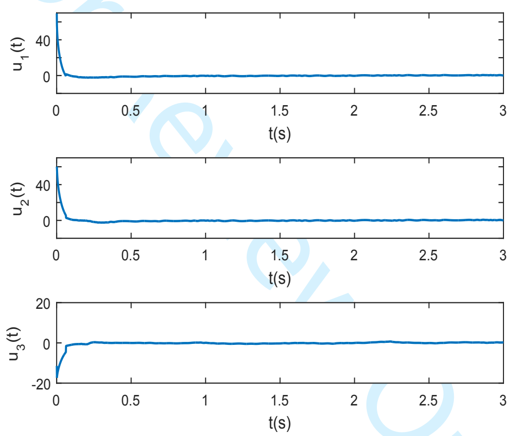

Fig. 6. The time history of the hybrid control inputs.

From figures (4) and (5) it can be seen that the synchronization errors converge to zero in a short time without any overshoot and steady state error. In order to compare the result of the synchronization of FO chaotic Chen systems (47) and (48) based on the controllers (35), (39), and the hybrid controller designed in this section, as well as the results of the synchronization based on [32, 33], an appropriate cost function is considered as $J = (1/N)\sum_{i=1}^{N}\left(\sum_{j=1}^{3} e_j(i)^2 + u_j(i)^2\right)^{0.5}$; where N is the time of simulation divided by h. One can see from Table 1 that, the proposed hybrid control technique is more efficient versus the different initial conditions and also has the better result against the control inputs designed in the some of the previous papers such as [32, 33].

***	Controller 1 (35)	Controller 2 (39)	Hybrid Controller	Controller [32]	Coupling method[33]
x(0)=[1.5 0.1 1.7], y(0)=[0.5 1.4 0.2]	1.5162	2.4745	1.4428	1.5445	11.7045
x(0)=[0.2 0.5 0.4], y(0)=[0.9 1.1 0.6]	0.6898	0.7567	0.6656	0.7562	1.2730
x(0)=[2 1.6 1.4], y(0)=[2.2 0.4 1.5]	1.1814	1.5962	1.0909	1.2275	1.8394

Table 1: The cost function values based on the different control input signals

5. Conclusion

In this paper, the stabilization and synchronization problems of identical FO chaotic systems are investigated. A new hybrid FO sliding mode controller is introduced that is robust against perturbations. Two illustrative examples show the feasibility and applicability of the proposed control techniques. For further studies, we ask the readers to investigate a way to obtain a sub-optimal control law for the control and synchronization of such FO complex chaotic systems as well as non-identical FO real chaotic and hyper-chaotic systems. Also, one can obtain the parameter Q adaptively to minimize the cost function in the real time and it is an open problem.

Acknowledgement. N. Pariz (the corresponding author) was supported by a grant from Ferdowsi University of Mashhad (No. 45123).

References

[1] Podlubny, I., *Fractional differential equations*, Academic Press, San Diego (1999).

[2] Kiani-B, A., Fallahi, K., Pariz, N., Leong, H. "A chaotic secure communication scheme using fractional chaotic systems based on an extended fractional Kalman filter," *Commun. Nonlinear Sci. Numer. Simul.*, Vol. 14, pp. 863-879 (2009).

[3] Kuntanapreeda, S. "Tensor product model transformation based control and synchronization of a class of fractional-order chaotic systems," *Asian J. Control*, Vol. 17, pp. 371–380 (2015).

[4] Dadras, S., Dadras, S., Malek, H., Chen, Y.Q. "A note on the Lyapunov stability of fractional order nonlinear systems," *Proceedings of the ASME 2017 International Design Engineering Technical Conferences and Computers and Information in Engineering Conference* (2017).

[5] Thuan, M.V., Huong, D.C. "New results on stabilization of fractional-order nonlinear systems via an LMI approach", *Asian J. Control*, Vol. 20, pp. 1–10 (2018).

[6] Mazinan, A.H., Kazemi, M.F., Shirzad, H. "An efficient robust adaptive sliding mode control approach with its application to secure communications in the presence of uncertainties, external disturbance and unknown parameters", Trans. Ins. Measure. Control, Vol. 36, pp. 164–174 (2014).

[7] Delavari, H., Mohadeszadeh, M. "Robust finite-time synchronization of non-identical fractional order hyperchaotic systems and its application in secure communication," *IEEE/CAA J. Auto. Sinica*, Vol. 3 (2016).

[8] Shutang, L., Fangfang, Z. "Complex function projective synchronization of complex chaotic system and its applications in secure communication," *Nonlinear Dyn.,* Vol. 76, pp. 1087-1097 (2014).

[9] Luo, C., Wang, X. "Chaos in the fractional-order complex Lorenz system and its synchronization," *Nonlinear Dyn.,* Vol. 71, pp. 241-257 (2013).

[10] Luo, C., Wang, X. "Chaos generated from the fractional-order complex Chen system and its application to digital secuer communication," *Int. J. Mod. Phys. C*, Vol. 24, pp. 1-23 (2013).

[11] Liu, X.J., Hong, L., Yang, L.X. "Fractional-order complex T system: bifurcations, chaos control and synchronization," *Nonlinear Dyn.* Vol. 75, pp. 589-602 (2014).

[12] Jiang, C., Liu, S., Luo, C.A. "New fractional-order chaotic complex system and its anti-synchronization," *Hindawi*, DOI: http://dx.doi.org/10.1155/2014/326354 (2014).

[13] Pecora, L.M., Carroll, T. L. "Synchronization in chaotic systems," *Phys. Rev. Lett.,* Vol. 64, pp. 821-824 (1990).

[14] Mohadeszadeh, M., Karimpour, A., Pariz, N. "Synchronization of fractional-order complex systems and its application" *Pramana – J. Phys.,* Vol. 92, pp. 1-10 (2019).

[15] Mobayen, S., Tchier, F. "Synchronization of a class of uncertain chaotic systems with Lipschitz nonlinearities using state-feedback control design: A matrix inequality approach," *Asian J. Control*, DOI: 10.1002/asjc.1512. (2017).

[16] Aghababa, M. P. "Finite-time chaos control and synchronization of fractional-order non-autonomous chaotic (hyperchaotic) systems using fractional nonsingular terminal sliding mode technique," *Nonlinear Dyn.,* Vol. 69, pp. 247-261 (2012).

[17] Shahnazi, R., Pariz, N., Vahidian Kamyad, A. "Observer-based adaptive fuzzy control of time-delay uncertain nonlinear systems," *Asian J. Control*, Vol. 13, pp. 456-460 (2011).

[18] Mohadeszadeh, M., Delavari, H. "Synchronization of fractional-order hyper chaotic systems based on a new adaptive sliding mode control," *Int. J. Dynam. Control*, Vol. 5, pp. 124-134 (2017).

[19] Luo, R. Z., Wang, Y. L. “Finite-time modified projective synchronization between two different chaotic systems with parameter and model uncertainties and external disturbances via sliding control,” *Indian J. Phys*., Vol. 88, pp. 301–309 (2014).

[20] Mardani, M. M., Vafamand, N., Shokrian Zeini, M., Shasadeghi, M., Khayatian, A. “Sum-of-squares-based finite-time adaptive sliding mode control of uncertain polynomial systems with input nonlinearities,” *Asian J. Control*, Vol. 20, pp. 1-5 (2018).

[21] Dadras, S., Momeni, H. R. “Control of a fractional-order economical system via sliding mode,” *Physica A*, Vol. 389, pp. 2434–2442 (2010).

[22] Lee, H., Utkin, V.I. “Chattering suppression methods in sliding mode control systems,” *Ann. Rev. Control*, Vol. 31, pp. 179–188 (2007).

[23] Nemati, H., Bando, M., Hokamoto, S. “Chattering attenuation sliding mode approach for nonlinear systems,” *Asian J. Control*, Vol. 19, pp. 1–13 (2017).

[24] Dadras, S., Momeni, H. R. “LMI-Based fractional integral sliding-mode control of uncertain nonlinear systems,” *Journal of Dynamic Systems, Measurement and Control*, (2014).

[25] Sun, J., Shen, Y., Zhang, X. “Modified projective and modified function projective synchronization of a class of real nonlinear systems and a class of complex nonlinear systems,” *Nonlinear Dyn*. Vol. 78, pp. 1755-1764 (2014).

[26] Zhendong, S., Shuzhi, S. G. *Switched Linear Systems; Control and Design*, (2005).

[27] Diethelm, K., Ford, N.J., Freed, A.D. “A predictor-corrector approach for the numerical solution of fractional differentia equations,” *Nonlinear Dyn.* Vol. 29, pp. 3-22 (2002).

[28] Chun, Y., Dadras, S., Zhong, S.M., Chen, Y.Q. “Control of a novel class of fractional-order chaotic systems via adaptive sliding mode control approach,” *Applied Mathematical Modelling,* Vol. 37, pp. 2469–2483 (2013).

[29] Khalil, H.-K., *Nonlinear System*. Third ed., Prentice Hall, New Jersey (2002).

[30] Aguila-Camacho, N., Duarte-Mermoud, M.A., Gallegos, J.A. “Lyapunov functions for fractional order systems,” *Commun. Nonlinear Sci. Numer. Simul*. Vol. 19, pp. 2951-2957 (2014).

[31] Li, C., Chen, G. “Chaos in the fractional order Chen system and its control,” *Chaos, Solitons and Fractals*, Vol. 22, pp. 549–554 (2004).

[32] Wang, J., Xiong, X., Zhang, Y. “Extending synchronization scheme to chaotic fractional-order Chen systems,” *Physica A*, Vol. 370, pp. 279–285 (2006).

[33] Zhu, H., Zhou, S., He, Z. “Chaos synchronization of the fractional-order Chen’s system,” *Chaos, Solitons and Fractals,* Vol. 41, pp. 2733–2740 (2009).

Dear Editor and Reviewers

The authors of the paper would like to thank Editor and Reviewers for her/his insightful comments. We have highlighted the comment in the paper by blue ink. We now respond to the point raised:

Reviewer 1's Comment :

The quality of the paper has improved a lot and content is publishable in this condition.

There is only a minor concern:

The referencing method is not correct:

Kiani-B, A., K. Fallahi, N. Pariz, H. Leong, "A chaotic secure communication scheme using fractional chaotic systems based on an extended fractional Kalman filter," Commun. Nonlinear Sci. Numer. Simul., Vol. 14, pp. 863-879 (2009).

The order of the first name and last name for all authors should be the same like:

Kiani-B, A., Fallahi, K., Pariz, N., Leong, H. "A chaotic secure communication scheme using fractional chaotic systems based on an extended fractional Kalman filter," Commun. Nonlinear Sci. Numer. Simul., Vol. 14, pp. 863-879 (2009).

Respond to the reviewer comment:

The order of the first name and last name for all authors in the references are improved by blue ink.

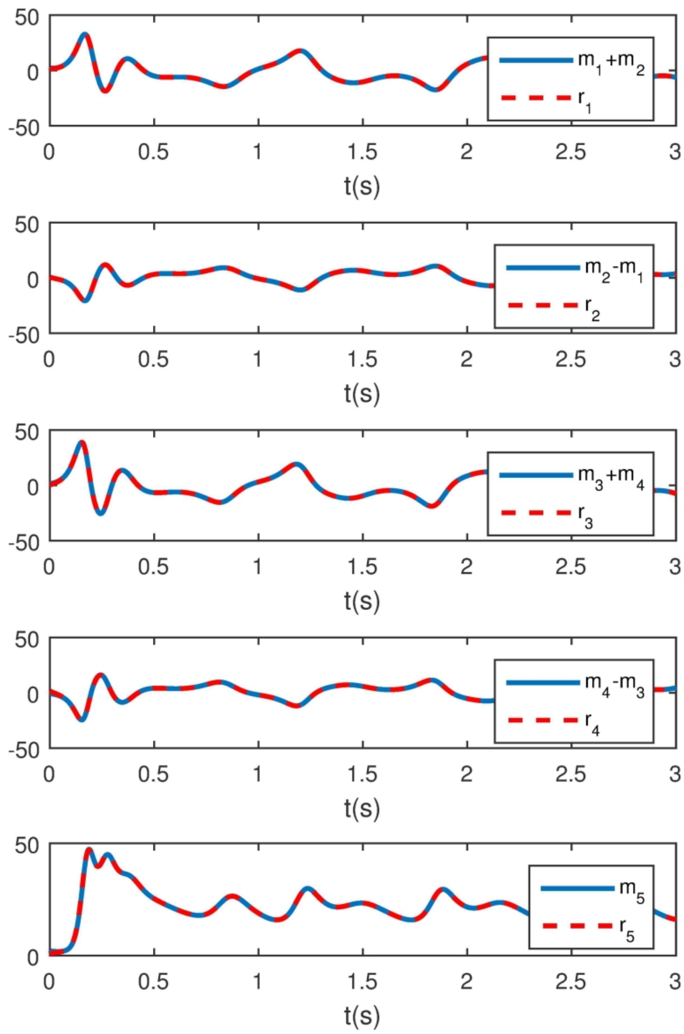

Fig. 1. The synchronized states of two identical FO complex chaotic Chen systems.

183x272mm (300 x 300 DPI)

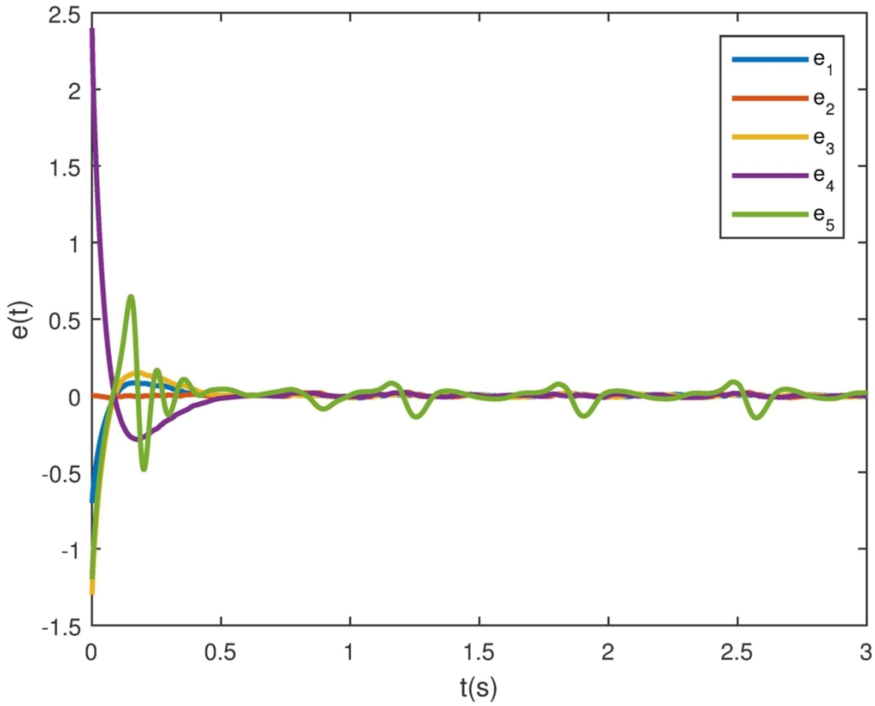

Fig. 2. The synchronization errors between the system (43) and system (44).

111x83mm (300 x 300 DPI)

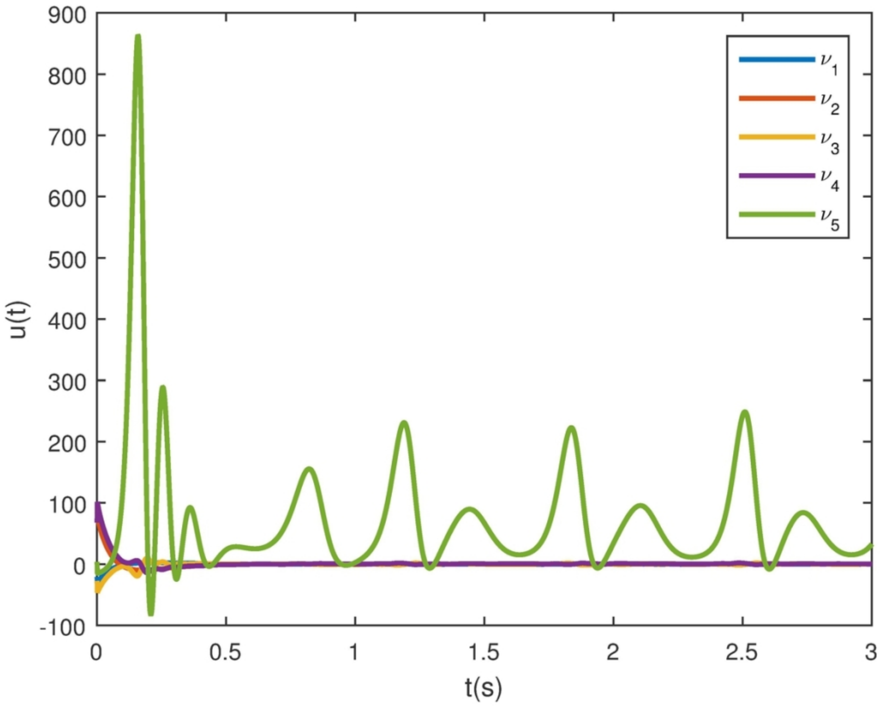

Fig. 3. The time history of control inputs (26).

111x83mm (300 x 300 DPI)

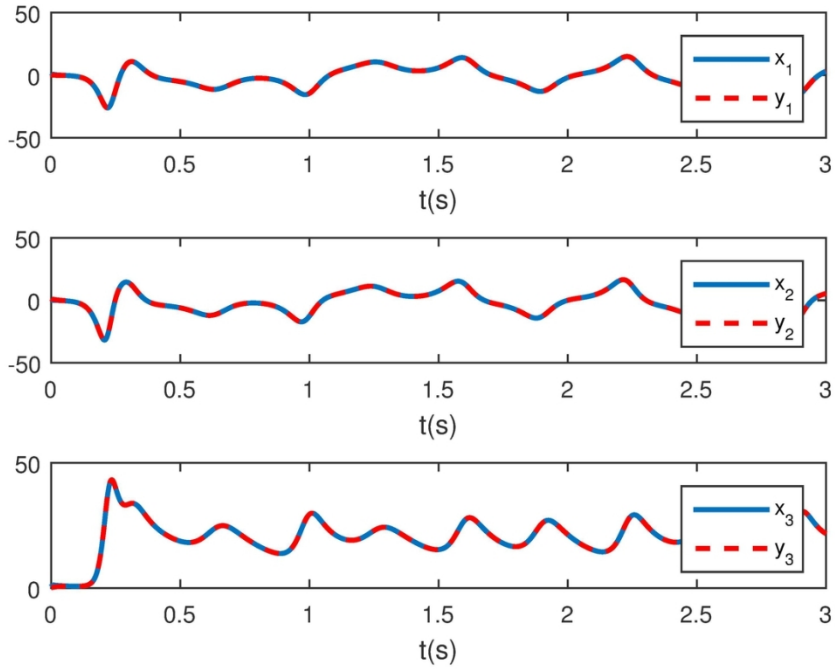

Fig. 4. The synchronized the sates of the system (47) and system (48).

111x83mm (300 x 300 DPI)

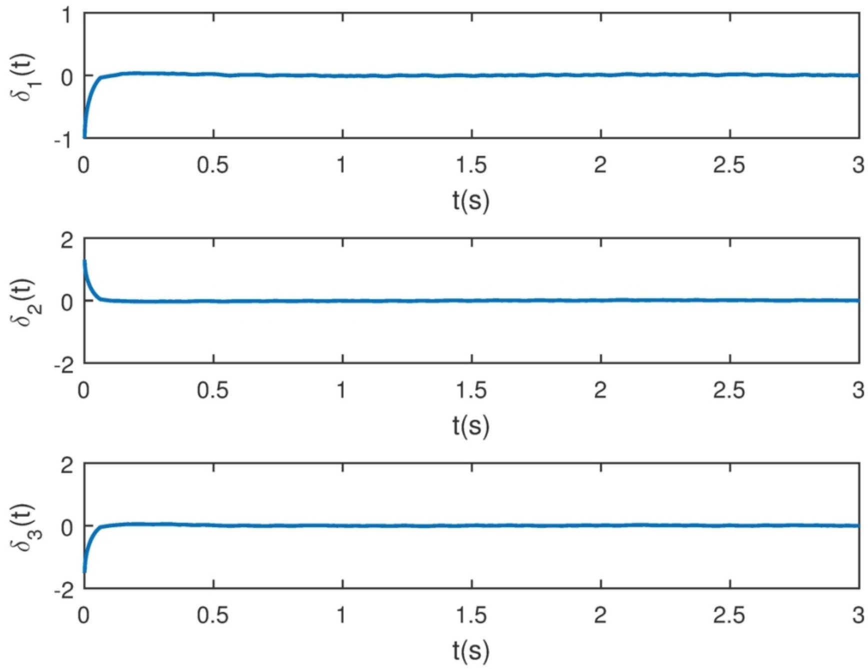

Fig. 5. The synchronization errors between the system (47) and system (48).

111x83mm (300 x 300 DPI)

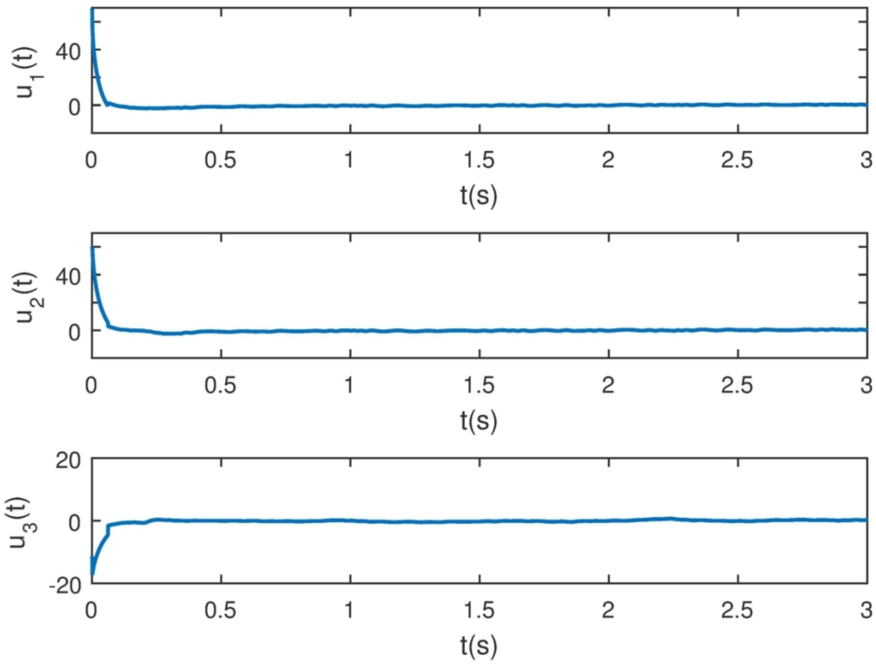

Fig. 6. The time history of hybrid control inputs.

111x83mm (300 x 300 DPI)